

Supporting Information for
Mechanisms of Se(IV) Incorporation in Jarosite and the Migration
Behavior During Thermal Aging

Yi Tan,^{1,2,3,†} Shiyin Ji,^{1,2,†} Renren Wang,^{1,2,4} Zitong Yan,^{1,2} Shouye Liu,^{1,2} Zhiwei Mou,^{1,2}

Yawen Liu,^{1,2,3} Guangyuan Chen,^{1,2,3} Tao Duan,^{1,2} Lin Zhu^{1,2}*

¹ National Co-Innovation Center for Nuclear Waste Disposal and Environmental Safety, Southwest University of Science and Technology, Mianyang 621010, China

² State Key Laboratory of Environment-friendly Energy Materials, School of National Defense Science & Technology, Southwest University of Science and Technology, Mianyang 621010, China

³ School of Environment and Resource, Southwest University of Science and Technology, Mianyang, Sichuan 621010, China

⁴ School of Materials and Chemistry, Southwest University of Science and Technology, Mianyang, Sichuan 621010, China

*Corresponding Authors Email: zhulin@swust.edu.cn (Lin Zhu)

† These two authors contributed equally

Contents

Section S1. Chemicals.

Section S2. Synthesis of Jarosite, Jarosite-Se(IV), Jarosite-Se(IV)-Aging.

Section S3. Batch experiments.

Section S4. Zeta potential measurements.

Table S1. Fitting results of sorption isothermal models.

Table S2. Fitting results of sorption kinetics models.

Table S3. Peak BE, FWHM, Atomic of phases presented in Jarosite, Jarosite-Se(IV), Jarosite-Se(IV)-Aging.

Figure S1. FT-IR spectral of Jarosite, Jarosite-Se(IV), Jarosite-Se(IV)-Aging.

Figure S2. The crystal structure of (a) Jarosite, (b) Hematite, (c) Ferric selenite.

Figure S3. Powder X-ray diffraction (PXRD) patterns of jarosite after immersed in aqueous solution with different pH values ranging from 2 to 11.

Figure S4. Powder X-ray diffraction (PXRD) patterns of jarosite sample before and after 150 days.

Figure S5. Zeta-potential values of jarosite in water under pH 2-11.

Figure S6. (a) The concentration of SO_4^{2-} changes as a function of pH during Se(IV) sorption process and leaching (blank) text. (b) pH changes during Se(IV) sorption and leaching text under different acid-base conditions.

Figure S7. Order kinetics model fitting for Se(IV) by jarosite.

Figure S8. Sorption thermodynamic model fitting for Se(IV) by jarosite.

Figure S9. (a) High resolution XPS spectra of C1s for (a) Jarosite, (b) Jarosite-Se(IV), (c) Jarosite-Se(IV)-Aging and O1s for (d) Jarosite-Se(IV)-Aging.

Figure S10. The concentration of Se(IV) during thermal aging.

Section S1. Chemicals.

KOH (> 95 % purity, CAS: 1310-58-3), $\text{Fe}_2(\text{SO}_4)_3 \cdot 5\text{H}_2\text{O}$ (> 97 % purity, CAS: 142906-29-4), HNO_3 (65–68 %, CAS: 7697-37-2), NaOH (97 % purity, CAS: 1310-73-2). All the chemicals were of analytical grade and used without any further treatment.

Section S2. Synthesis routes of Jarosite, Jarosite-Se(IV), Jarosite-Se(IV)-Aging.

Jarosite. 5.6 g of KOH was added to 17.2 g of $\text{Fe}_2(\text{SO}_4)_3 \cdot 5\text{H}_2\text{O}$ in 100 mL of deionized water, and then continuously stirring at 95 °C for 4 h. After heating down, the resulting precipitate was rinsed with deionized water several times. The filtered sediment was put into a 60 °C oven to dry for 24 h, the dried solid was ground into powder to obtain jarosite sample.

Jarosite-Se(IV). After the synthesis of jarosite, 40 mg of the synthesized jarosite and 20 mL of 500 mg/L Se(IV) were mixed in glass bottles and adsorbed for 12 hours (Make sure the pH of the solution was 10 and the ionic strength of the solution was 0.01 M NaNO_3). The mixed solution was adsorbed for 12 hours and transferred into stainless steel autoclave at 180 °C for 3 days. Finally, the filtered sediment was put into the freeze dryer for 48 hours to obtain the sample.

Jarosite-Se(IV)-Aging. Take three parts of the adsorbed mixture under the same conditions (first paragraph in **Section S2**), and then transferred the mixture into high-pressure reactor at 180 °C for 3 days. After cooling down, the aged solution was filtered and the sediment was freeze-dried to obtain the aged sample.

Section S3. Batch experiments.

All the experiments were conducted at room temperature (25 °C). In all sorption experiments, the solid/liquid ratio was 2 g/L. Typically, 20 mg jarosite was added to 10 mL solution with a certain concentration of Se(IV). For controlling the ionic strength,

0.01 M NaNO₃ was used as the background electrolyte. All pH values were adjusted with HNO₃ (0.01 M to 1 M) and NaOH (0.01 M to 1 M). The resulting mixture was magnetic stirred and separated with a 0.22 μm membrane filter. The concentrations of selenium in aqueous solution were determined by Inductively Coupled Plasma Optical Emission Spectrometry (ICP-OES) and Inductively Coupled Plasma Mass Spectrometry (ICP-MS).

Sorption under different pH values. Jarosite was added to a series of selenium solutions with same concentration (500 mg/L) and different pH values (from 2 to 11), the resulting mixtures were stirred for 24 hours. The concentrations of Se(IV) in mother liquors and solutions after contacting were determined by ICP-OES.

Sorption isotherms. Jarosite was added to a series of solutions with different concentration (from 10 mg/L to 500 mg/L) for Se(IV) and initial pH of 10, the resulting mixtures were stirred for 24 hours. The concentrations of mother liquors and solutions after contacting were determined by ICP-OES.

Sorption kinetics. 200 mg jarosite was added to 100 mL solution with concentration of 500 mg/L for Se(IV) and an initial pH value of 11. For measuring the concentration of Se(IV) in the solution, no background electrolyte was added. HNO₃ (0.01 M to 1 M) and NaOH (0.01 M to 1 M) were used to adjust the pH. The resulting mixture was magnetic stirred thoroughly. At specific time point (from 5 min to 720 min), a small amount of aqueous solution was filtered and diluted 50 times, the selenium and sulfur concentration of which was determined by ICP-OES.

Sorption under different Ionic strength. Jarosite was added to the solution with an initial concentration of 500 mg/L Se(IV), the initial pH values were 7 and 11, and the ionic strength of the solution NaNO₃ was controlled to be 0 mM, 0.01 mM, 0.05 mM and 0.1 mM, respectively. The adsorbed mixture was stirred for 24 h, and the

concentration of Se(IV) in mother solution and adsorbed solution was determined by inductively coupled plasma emission spectrometer (ICP-OES) after filtration.

Removal efficiency under competitive anions. Solutions with same selenium concentration of 1 mg/L (0.0125 mM) and different competitive anions composition of 0.1 mM Cl⁻, 0.1 mM NO₃⁻, 0.3 mM CO₃²⁻, 0.1 mM SO₄²⁻, 0.1 mM HPO₄²⁻ and all five anions (the concentration of each is same with the single anion experiments) were prepared. Jarosite was added to above solutions and stirred for 24 hours. The removal efficiency was calculated from the selenium concentration of solution after contacting determined by ICP-MS.

Section S4. Zeta potential measurements.

20 mg of jarosite were added into a beaker containing 100 mL of deionized water and ultrasound for 5min. The mixture was added into 10 glass bottles after ultrasound, respectively. After that, the pH of each bottle was adjusted to 2, 3, 4, 5, 6, 7, 8, 9, 10, 11 within 5 min. Finally, the adjusted solution was used to measure the Zeta potential.

Table S1. Fitting results of sorption kinetics models.

Samples	Q _{e(exp)} (mg/g)	Pseudo-first-order			Pseudo-second-order		
		K ₁ (1/min)	q _e (mg/g)	R ²	K ₂ (g/mgmin)	q _e (mg/g)	R ²
Jarosite	40	1.9×10 ⁻³	23.48	0.83	3.36×10 ⁻⁴	39.15	0.998

Table S2. Fitting results of sorption isothermal models.

Samples	Langmuir			Freundlich		
	q _m (mg/g)	K _L (L/mg)	R ²	k _F (mg/g)	n	R ²
Jarosite	31.71	0.013	0.435	3.353	4.61	0.658

Table S3. Peak BE, FWHM, Atomic of phases in Jarosite, Jarosite-Se(IV), Jarosite-Se(IV)-Aging.

Survey of Jarosite, Jarosite-Se(IV), Jarosite-Se(IV)-Aging			
Jarosite	Name	Peak BE	Atomic %
	O1s	531.41	74.49
	Fe2p	711.92	8.56
	K2p	292.51	5.05
	S2p	168.28	11.90
Jarosite-Se(IV)	Name	Peak BE	Atomic %
	O1s	531.37	54.93
	Se3d	57.23	6.84
	Fe2p	711.76	10.33
	S2p	168.59	10.08
	K2p	292.47	3.91
Jarosite-Se(IV)-Aging	Name	Peak BE	Atomic %
	O1s	531.37	58.05
	Fe2p	711.43	24.72
	S2p	164.09	1.62
	Se3d	58.11	13.59
	K2p	292.37	2.03

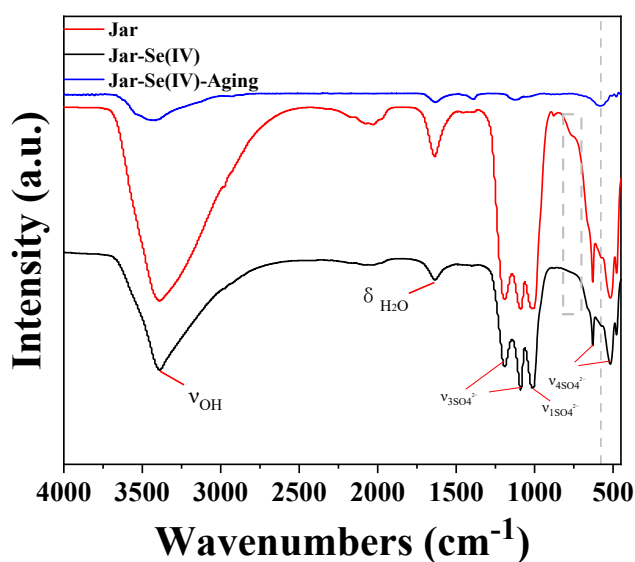


Figure S1. FT-IR spectral of Jarosite, Jarosite-Se(IV), Jarosite-Se(IV)-Aging

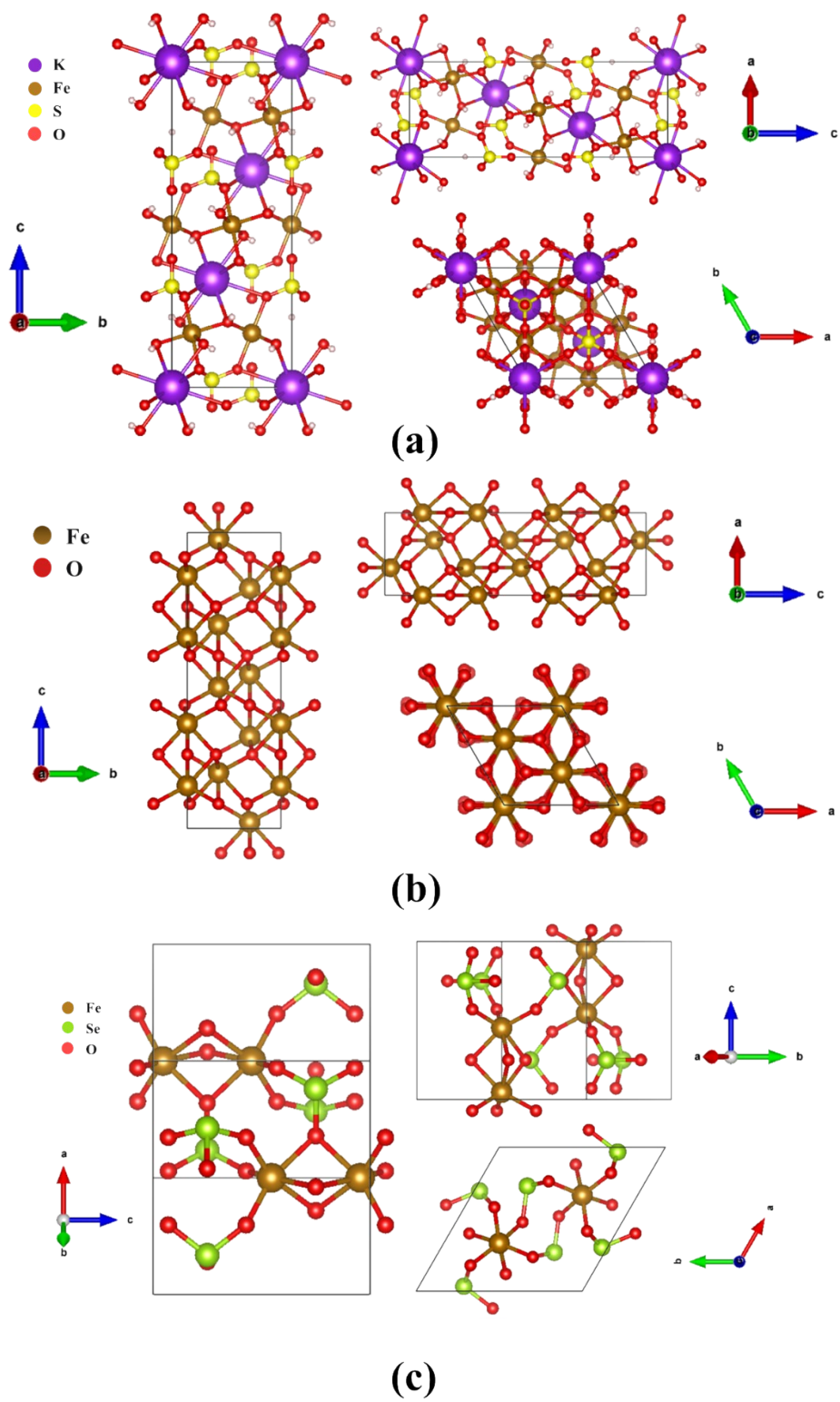


Figure S2. The crystal structure of (a) Jarosite, (b) Hematite. (c) Ferric selenite

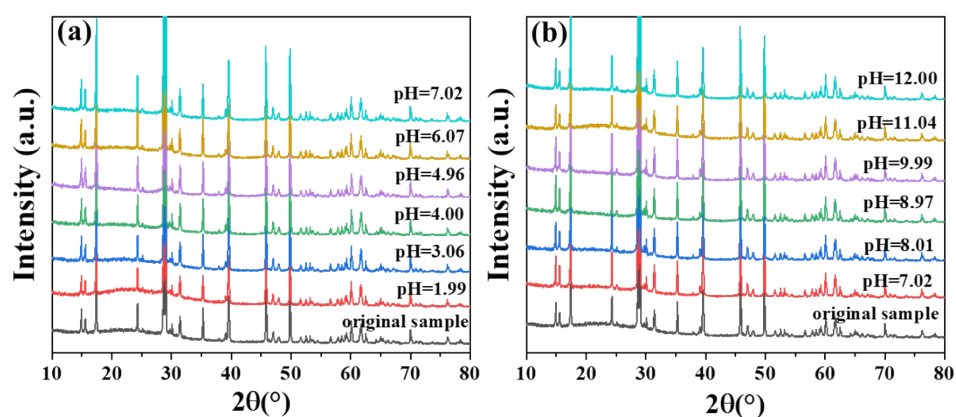


Figure S3. Powder X-ray diffraction (PXRD) patterns of jarosite after immersed in aqueous solution with different pH values ranging from 2 to 11.

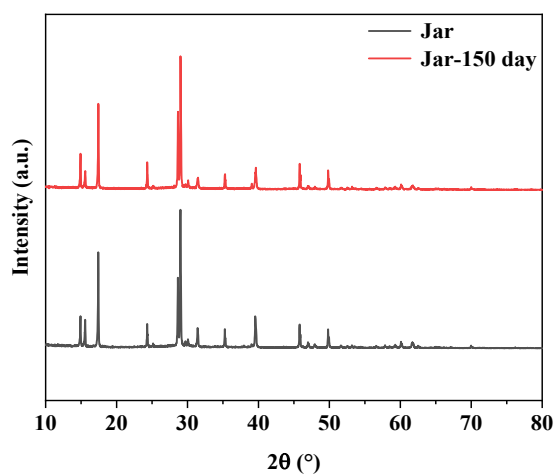


Figure S4. Powder X-ray diffraction (PXRD) patterns of jarosite sample before and after 150 days.

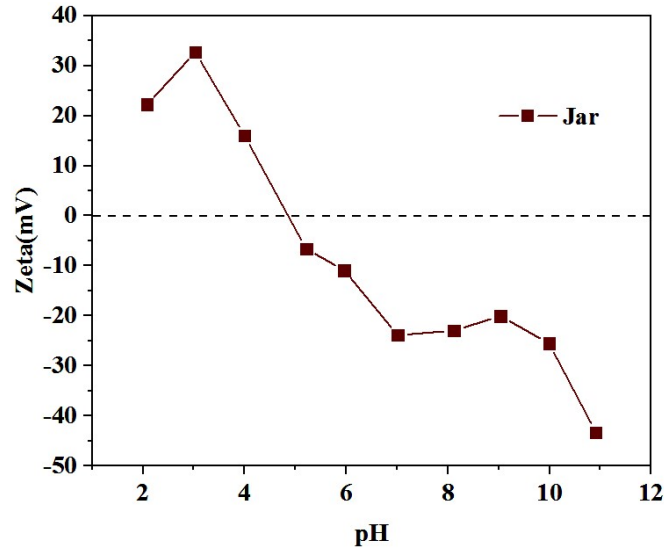


Figure S5. Zeta-potential values of jarosite in water under pH 2-11.

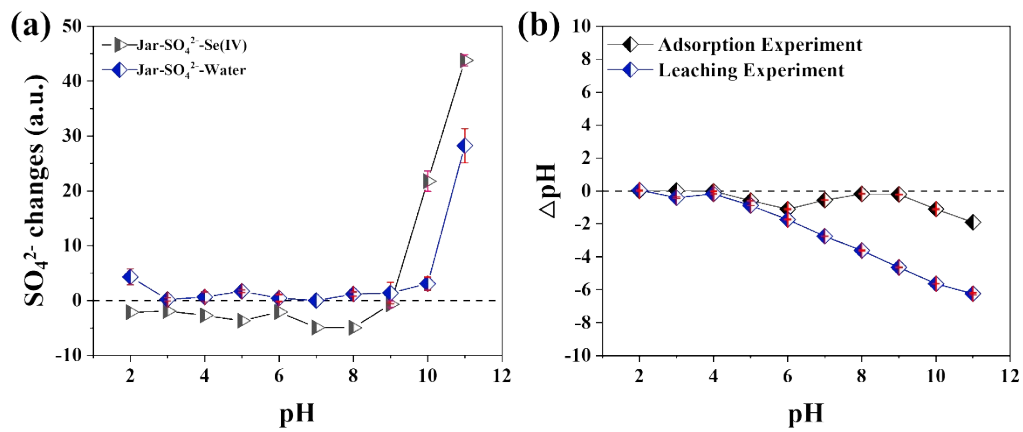


Figure S6. (a) The concentration of SO_4^{2-} changes as a function of pH during Se(IV) sorption process and leaching (**blank**) text. (b) pH changes during Se(IV) sorption and leaching text under different acid-base conditions.

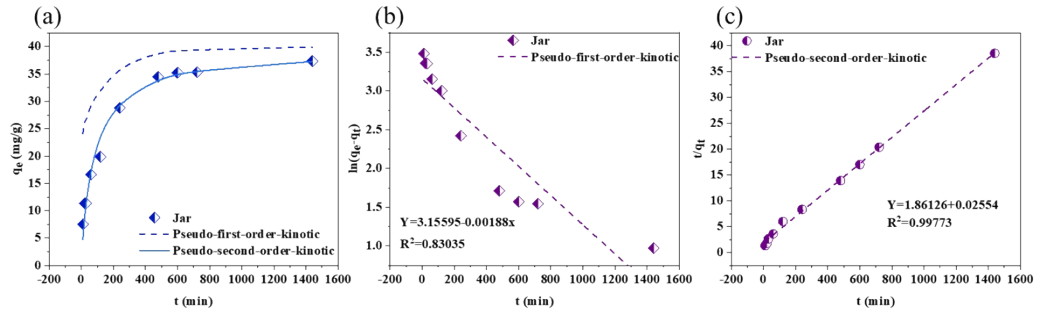


Figure S7. Order kinetics model fitting for Se(IV) by jarosite.

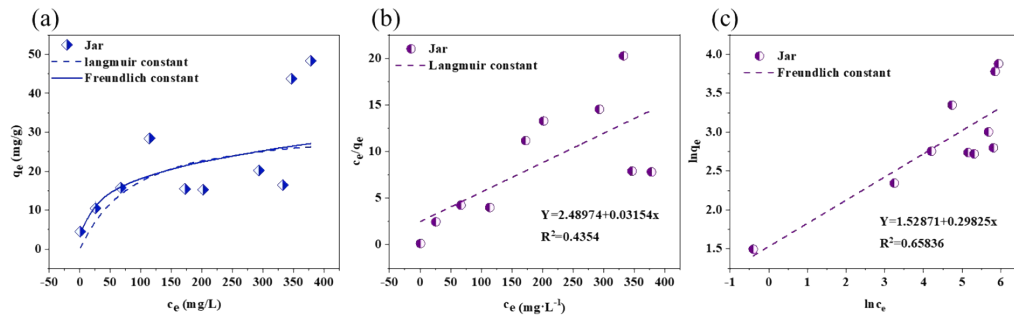


Figure S8. Sorption thermodynamic model fitting for Se(IV) by jarosite.

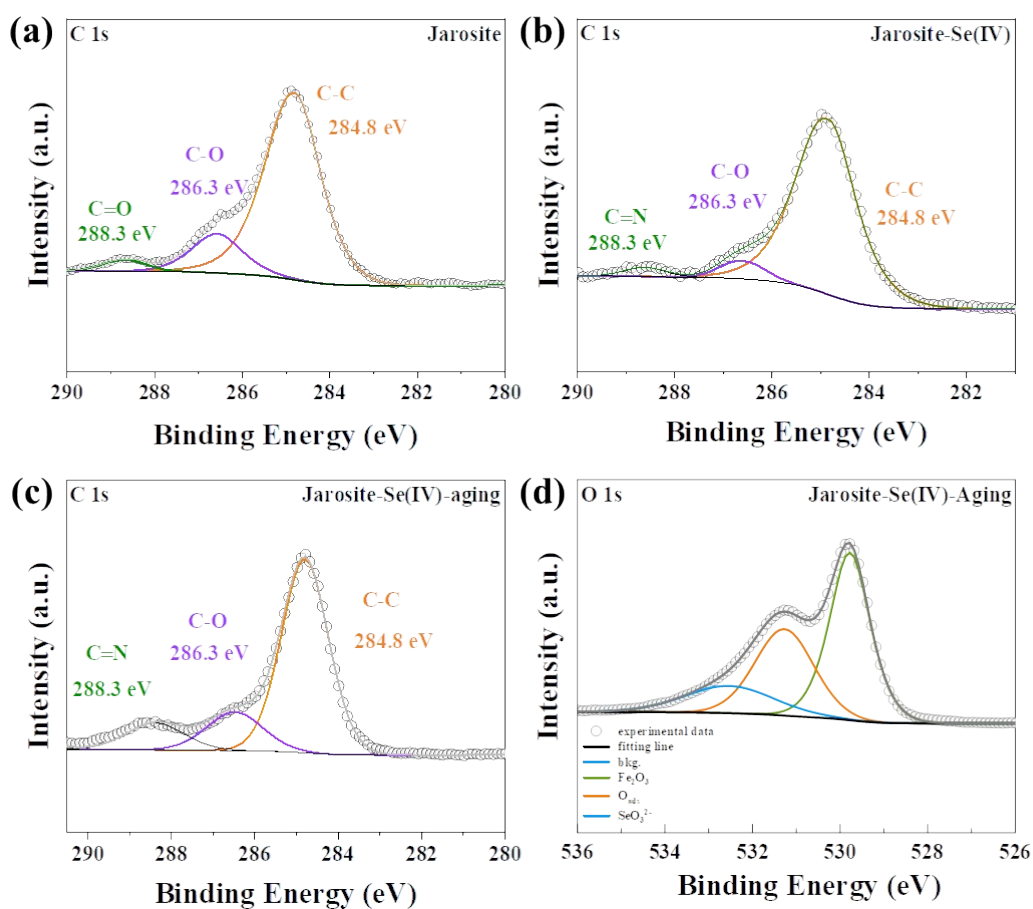


Figure S9. (a) High resolution XPS spectra of C1s for (a) Jarosite, (b) Jarosite-Se(IV), (c) Jarosite-Se(IV)-Aging and O1s for (d) Jarosite-Se(IV)-Aging.

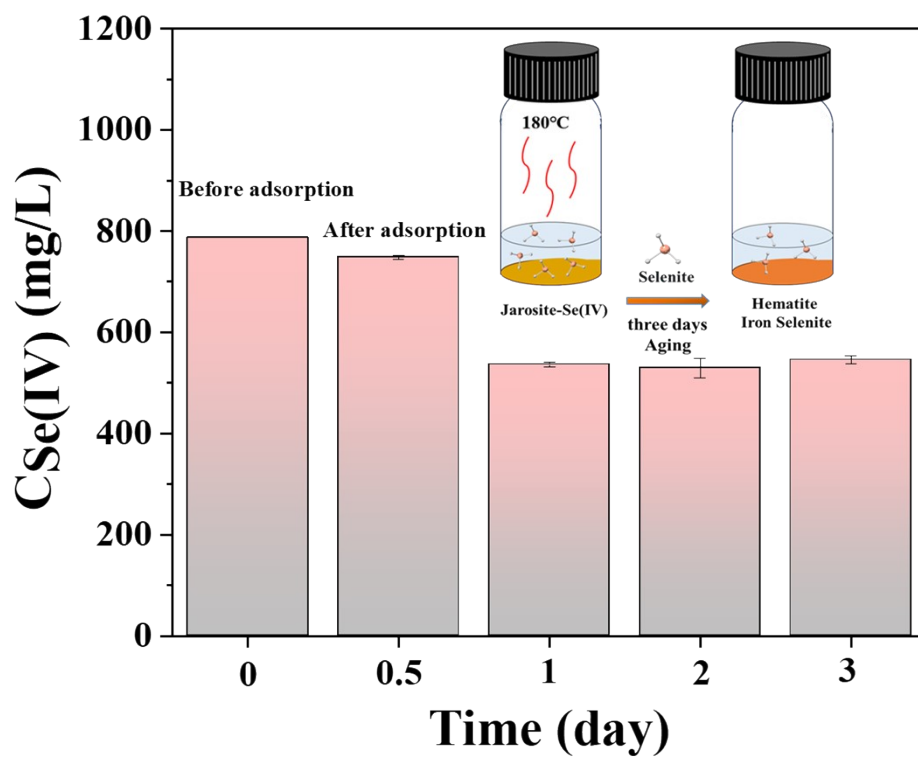


Figure S10. The concentration of Se(IV) during thermal aging.